

## CLEAN-UP OF WASTES FROM THE TEXTILE INDUSTRY USING ANIONIC CLAYS

JORGE FLORES<sup>1</sup>, ENRIQUE LIMA<sup>2,\*</sup>, MARISELA MAUBERT<sup>1</sup>, ENRIQUE ADUNA<sup>1</sup>, AND JOSE LUIS RIVERA<sup>2</sup>

<sup>1</sup> Universidad Autónoma Metropolitana, Azcapotzalco, Av. San Pablo 180, Col. Reynosa Tamaulipas, 02200 México D.F., México

<sup>2</sup> Instituto de Investigaciones en Materiales, Universidad Nacional Autónoma de México, Circuito exterior s/n, Cd. Universitaria, Del. Coyoacán, CP 04510, México D.F., Mexico

**Abstract**—Toxic dyes must be removed from waste water coming from the textile and paint industries. Adsorption is one possible method of removing dyes under ‘soft’ conditions, without the generation of secondary hazardous materials. The present study used the carbonate-containing layered double hydroxides (LDH), Mg–Al and Mg–Zn–Al (with a  $M^{2+}/M^{3+}$  ratio of 3), as adsorbents to remove two industrial colorants, Astrazon Remazol Brilliant Blue and Direct Red, present in low concentrations in aqueous solutions. The physicochemical properties of adsorbents at the surfaces of LDH, as well as the properties of the solutions containing the dyes control how the colorants are removed. Both fresh and calcined LDH were effective in the removal experiments, with effectiveness ranging from 50 to 100%. Analysis of kinetic data demonstrated that the adsorption process fitted the pseudo-second-order model better than the pseudo-first order model, information which is useful for system design in the treatment of wastes from the textile industry. Parameters such as pH of solutions and concentration of dye in solution influenced mainly the initial adsorption rate.

**Key Words**—Adsorption, Colorant, Dyes, Hydrotalcite, Layered Double Hydroxides, Remediation, Textile Industry, Wastes.

### INTRODUCTION

The world’s colorant industry has seen production increase significantly in recent years. New dyes and pigments have been produced which are ‘eco-friendly’ but many dyes (organic and inorganic) are toxic and present in wastes from the textile industry, among others (Jones, 1967; El Molla and Schneider, 2006; Deligeorgiev *et al.*, 1995). Reactive dyes are used mainly for coloring cotton and cellulosic and blended fibers (Herbst and Hunger, 2004; Vigo, 1994). The pollution of water bodies is primarily due to non-biodegradable dyes along with the presence of toxic trace metals, acids, alkalis, and carcinogenic aromatic amines in the effluents (Choudhury, 2006). Pollutants associated with direct dyes are salts, unfixed dyes, copper salts, and cationic fixing agents.

Many organic colorants, in particular, are soluble in water, and these need to be removed in order to avoid propagation of the pollution. Removal by filtration or other physical methods is difficult. Some alternatives to remove this type of effluent involve the destruction of the pollutant molecules by means of chemical reactions or their retention in inorganic matrices (Santos *et al.*, 2008; Tunç *et al.*, 2009). The hosting chromophore molecules in inorganic matrices are not just used to treat polluted water effluents, but also in the preparation of

functional materials with many potential applications such as optical lasers or hybrid pigments (Ibarra *et al.*, 2005; Hsiue *et al.*, 1999). The selection of an inorganic matrix (adsorbent) depends on the physicochemical properties of the molecule to be sequestered. For example, the acidity and size windows of some molecular sieves are suitable for encapsulation of thioindigo molecules (Hoppe *et al.*, 1994; Wark *et al.*, 1998; Ganschow *et al.*, 1999). On the contrary, LDH, otherwise known as hydrotalcite-like compounds, HTs, are anionic exchangers and, therefore, able to retain methyl orange anions and other anionic dyes (Constantino *et al.*, 1999; Rives, 2002). Zeolites and HTs not only adsorb anionic species, they are also able to retain neutral molecules. The structural and surface properties of HTs are suitable for trapping some molecules with polar bonds. Azoic and betalain dyes are stabilized on the surfaces of HTs through strong interactions between the Al–O pairs of HTs and the functional groups such as N–H, C=O, and OR present in dyes (Laguna *et al.*, 2007; Lima *et al.*, 2009). In fact, the structure of HTs is based on  $M^{2+}(\text{OH})_6$  octahedral units sharing edges to build  $M^{2+}(\text{OH})_2$  brucite-like layers. A HT-like compound is created by partial isomorphous substitution of  $M^{2+}$  cations by trivalent cations with similar ionic radius, rendering a positively charged layer. This charge is compensated electrically by anionic species located in the interlayer region, along with hydration water molecules. The layer structure of HTs collapses if treated at temperatures as high as 400°C and emerges as a mixed oxide. If a Mg–Al–CO<sub>3</sub> HT is calcined at 400°C, the mixed oxide Mg(Al)O is obtained.

\* E-mail address of corresponding author:

lima@iim.unam.mx

DOI: 10.1346/CCMN.2011.0590303

Both layered HTs and mixed oxides have been used as sorbents, anion exchangers, drug-delivery carriers, PVC additives, and fire retardants (Figueras, 2004; Prinetto *et al.*, 2000a; Climent *et al.*, 2004). The structure of HTs is, therefore, suitable for trapping the dyes present in aqueous solutions. Some studies (*e.g.* Zhu *et al.*, 2005; El Gaini 2009; Orthman *et al.*, 2003) reported the adsorption of some dyes onto HT-like materials. Bouraada *et al.* (2009) proposed that Green Bezanyl-F2B dye can be removed from aqueous solutions using HTs as adsorbents. Modification of the adsorbent with sodium dodecylsulfate was necessary, however, to increase the absorption capacity of the HT. The carbonate-containing Mg-Al HT has been the most tested one as a potential adsorbent of dyes. Note, however, that effective retention of dye could occur on sorption sites (related to basicity or acidity) other than those offered by Mg-Al hydrotalcites. The present study was undertaken to discover the optimal HT adsorbents, with different compositions, to retain two specific industrial colorants present as pollutants in wastes from the textile industry. The effects of solution pH and the initial nature of the sorbent on the kinetics of removal were taken into consideration. The work focused mainly on kinetics aspects, as they can be crucial in the design of wastewater equipment for technological applications. Two reaction kinetics models were applied, pseudo first order and pseudo second order. One sorption diffusion model was also tested.

## EXPERIMENTAL

### Materials

Carbonate-containing MgAl HT with a Mg/Al atomic ratio of 3 was prepared by coprecipitation at pH 10, by simultaneous, dropwise addition of a solution A containing appropriate amounts of Mg and Al nitrates and a caustic solution B containing 1 M NaOH and 1 M Na<sub>2</sub>CO<sub>3</sub> solutions in distilled water.

The resulting white solid was washed repeatedly with hot distilled water and then dried at 80°C for 8 h. Another HT was prepared under similar conditions with Mg<sup>2+</sup> and Zn<sup>2+</sup> present simultaneously as divalent cations, while Al<sup>3+</sup> remained in the structure. The (Mg+Zn)/Al ratio was maintained at 3.

Mixed oxides were obtained by thermal treatment of HT materials under N<sub>2</sub> (100 mL min<sup>-1</sup>), with a heating rate of 10°C min<sup>-1</sup>, up to 450°C for 5 h. Mixed oxides were used after cooling to room temperature.

The nomenclature adopted was MgAl-HT and MgZnAl-HT for HTs, and (MgAl)O and (MgZnAl)O for mixed oxides.

### Characterization

**X-ray diffraction.** Powder X-ray diffraction (XRD) patterns were obtained using a Phillips X'PERT PRO powder diffractometer with a copper anode tube. The

CuK $\alpha$  radiation ( $\lambda = 1.54186 \text{ \AA}$ ) was selected using a diffracted-beam monochromator.

**NMR spectroscopy.** <sup>27</sup>Al magic-angle spinning nuclear magnetic resonance (MAS NMR) spectra were acquired using a Bruker Avance II spectrometer operating at a frequency of 78.21 MHz. Spectra were acquired with short single pulses ( $\pi/12$ ) and repetition times of 0.5 s. The samples were spun at 10 kHz and the chemical shifts were referenced to a 1 M Al(Cl)<sub>3</sub> solution.

### Adsorption of dyes by HTs

The HTs were tested as adsorbents of dyes Astrazon Remazol Brilliant Blue (ARBB) and Direct Red (DR) at 25°C, chemical structures of which are shown (Figure 1a,b). Adsorbents were used either in their layered form (uncalcined) or as mixed oxides (calcined at 450°C under N<sub>2</sub>). Typically, 100 mg of fresh or calcined solid was suspended in 100 mL of aqueous dye solution, and the retention of dye by the solid was monitored as a function of time. A Spectronic 20 Genesys spectrometer (Thermo Electron Scientific, Madison, Wisconsin, USA) was used to quantify the remaining dye in solution by UV-vis spectroscopy, converting observed absorbance values to concentration by means of a previously determined calibration curve using standard samples of ARBB and DR of known concentration in the range 0–100 ppm; both calibration curves were linear. The monitored UV-vis absorption bands were at wavelengths of 592 nm and 508 nm for ARBB and DR, respectively. The sorption of dyes onto HTs was carried out under different pH conditions (4, 5.9, and 8) and dye concentrations (25, 50, and 100 ppm). The pH

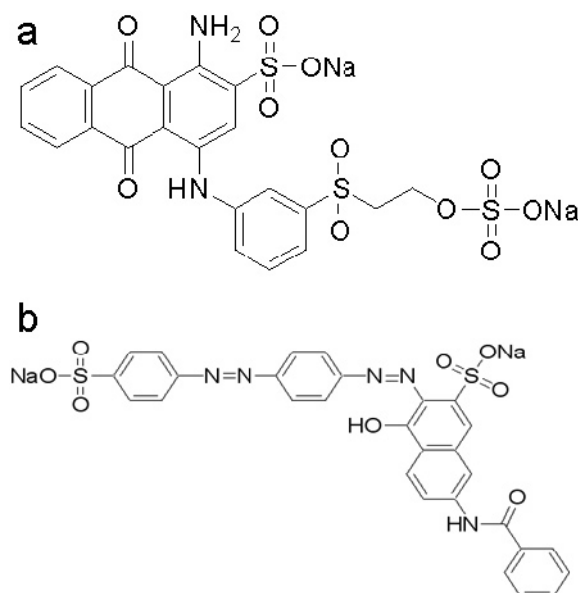


Figure 1. Chemical structures of (a) ARBB and (b) DR.

value was adjusted by adding NaOH or HNO<sub>3</sub> solutions. No buffer was used in order to avoid interference by other anions on the adsorption process.

## RESULTS AND DISCUSSION

### Adsorbents

The XRD traces (Figure 2a) showed that HT samples had a hydroxalite-like structure by fitting the diffraction pattern with the corresponding pattern from the Joint Committee on Powder Diffraction Standards (JCPDS). The average  $d_{003}$  distances were 7.67 Å for MgAl-HT and 7.63 Å for MgZnAl-HT, which fit with carbonated HTs (Johnson and Glasser, 2003; Thevenot *et al.*, 1989). The  $c = 3d_{003}$  parameter is indicative of the interlayer distance, and the  $a = 2d_{110}$  parameter is related to the average cation–cation distance in the brucite-like layers. Both parameters were obtained by Bragg's law assuming hexagonal stacking. As a result of the addition of Zn, the interlayer distances diminished due to an increase in the layer charge density (Zn is more electronegative than Al in terms of the Allred-Rochow electronegativities). Aluminum was incorporated into the octahedral part of the HT layers (Lippmaa *et al.*, 1986) as detected by the <sup>27</sup>Al NMR signal close to 5 ppm (Figure 3a). The absence of a signal in the 45–70 ppm range indicates the lack of tetrahedral Al species in these samples.

The layered structure collapsed with increasing temperature, leading to the formation of corresponding

(MgAl)O and (MgZnAl)O mixed oxides with a periclase-like structure, space group  $Fm\bar{3}m$ , as revealed by XRD (Figure 2b). For both calcined samples, the coordination of Al was partially lowered, from 6-fold to 4-fold, as shown by the appearance of an <sup>27</sup>Al NMR resonance close to 45 ppm (Figure 3b). No other crystalline phases were detected.

### Adsorption

*Parameters driving the adsorption.* The amount of ARBB adsorbed increased with contact time for all initial dye concentrations. For all adsorbents, dye removal was very quick; within 30 min at least half of the initial dye concentration had been removed, then a slow decrease over the following minutes was observed. For MgAl-HT, MgZn-HT, and mixed oxide MgZnAl(O) adsorbents, an adsorption time of ~100 min was sufficient to reach the equilibrium concentration. At this point, dye removal efficiencies were as high as 92% for initial concentrations as low as 25 and 50 ppm. In order to compare kinetic features in the same period of time, all experiments were monitored for up to 240 min. Note that from a system-design viewpoint, a lumped analysis of adsorption rates is sufficient for practical purposes (Wu *et al.*, 2001). Process performance and the ultimate cost of a sorption system have been shown to depend on the effectiveness of the process design and the efficiency of the process operation, which often require an understanding of the kinetics of uptake or the time

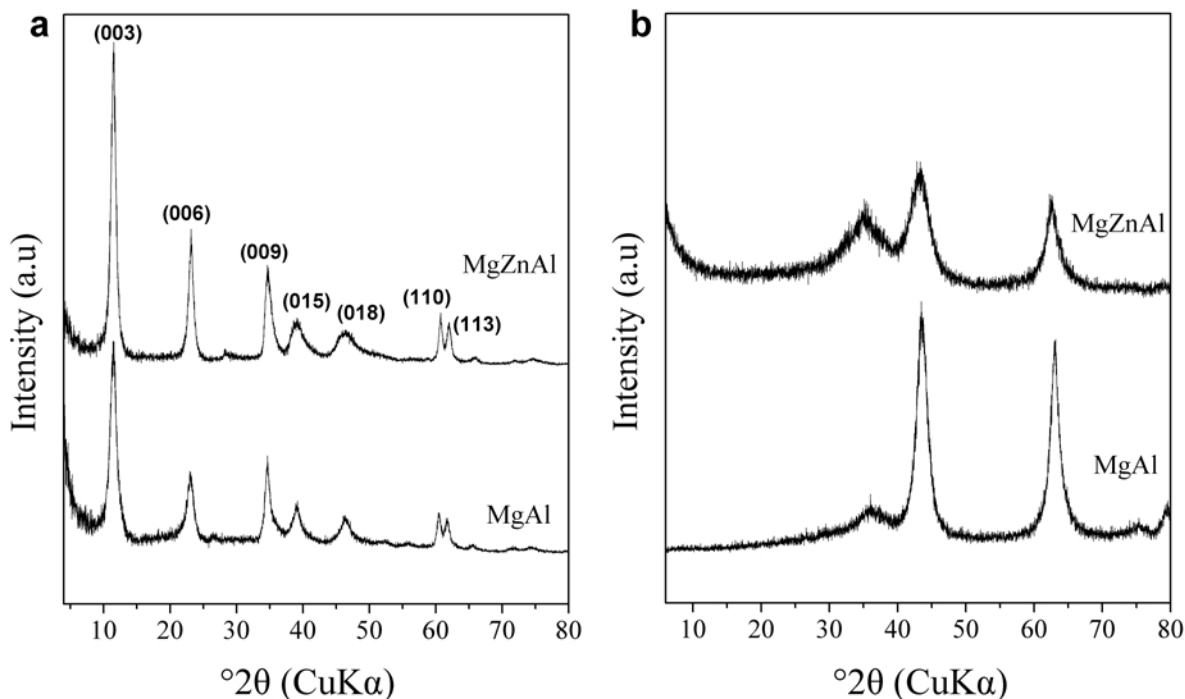


Figure 2. XRD patterns of (a) as-synthesized and (b) calcined HTs. Measurements were performed in air at room temperature with CuK $\alpha$  ( $\lambda = 0.15418$  nm) radiation at a scanning rate of  $1.2^\circ \text{min}^{-1}$  from  $2-80^\circ 2\theta$ .

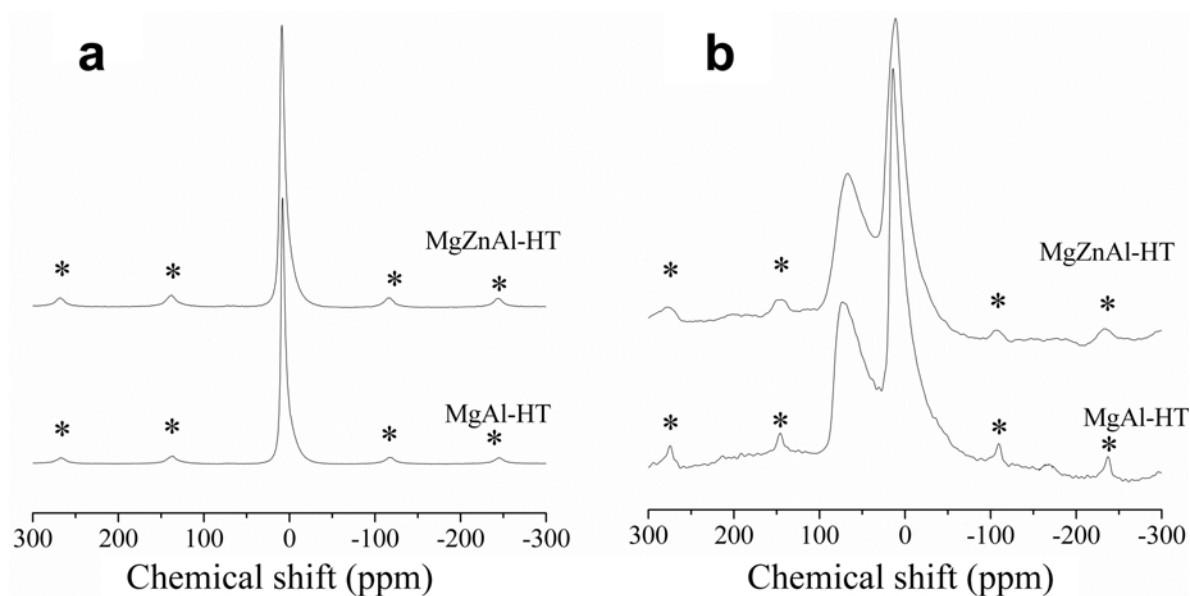


Figure 3.  $^{27}\text{Al}$  NMR spectra of adsorbents (a) as synthesized and (b) heated at  $450^\circ\text{C}$  for 5 h. \* indicates spinning side bands (10 kHz).

dependence of the concentration distribution of the solute by both bulk solution and by the solid adsorbent (Imbaraj *et al.*, 2006).

The present study elucidated first the equilibrium phenomena as mentioned above, then focused in detail

on the kinetic aspects. Curves showing the retention of ARBB onto the adsorbents, both calcined and uncalcined, were obtained (Figure 4). The concentration of dye in the starting solution, the presence of Zn in the adsorbent material, and the thermal treatment of the

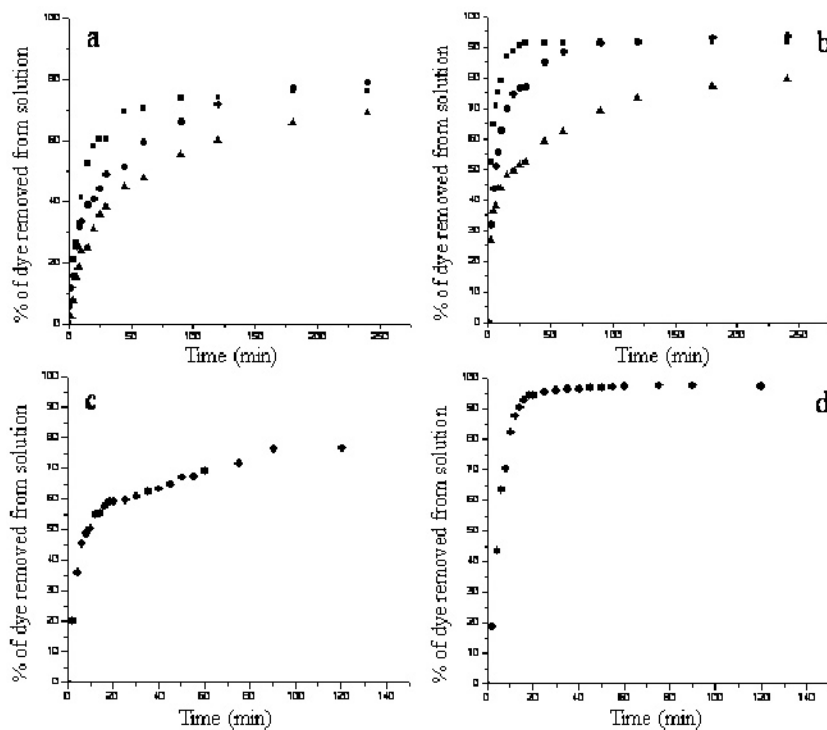


Figure 4. Amount of ARBB dye removed from solution with time by adsorbents: (a) MgAl-HT, (b) MgZnAl-HT, (c) MgAl-HT calcined at  $450^\circ\text{C}$  5 h, and (d) MgZnAl-HT calcined at  $450^\circ\text{C}$  5 h. Initial dye concentrations (ppm): 25 (■), 50 (●), and 100 (▲). All solutions at pH 5.9.

adsorbent clearly influence the kinetics of adsorption. The percentage of dye removed from solution through adsorption onto solids was determined by the concentration of dye in solution; the lower the dye concentration, the greater the percentage of dye removed by trapping onto the HT adsorbent, which was clearly observed for the uncalcined solids. Such a result is relevant because sometimes very large volumes of real wastes are produced with dye present in low concentrations. Such effluents could be cleaned using the adsorbents described, without the need for costly treatments such as evaporation. The presence of zinc in the HTs enhances the retention of dyes for any concentration of dye in solution considered here. Zinc is known to induce changes in the basicity of HTs (Rao *et al.*, 1998; Sampieri and Lima, 2009); a better performance of this material as an adsorbent of dyes with dipolar groups such as S=O, C=O, and N–H might be due to a chemical affinity between the dipolar groups and the Zn–O and Al–O pairs. On the other hand, calcined samples retain dyes more quickly than uncalcined samples, which might be due to the greater specific surface area of calcined samples (Valente *et al.*, 2009). Furthermore,  $^{27}\text{Al}$  NMR results showed that calcined samples have a large amount of 4-fold coordinated Al ( $^{\text{IV}}\text{Al}$ ), which can serve as an adsorption site better than 6-fold coordinated Al ( $^{\text{VI}}\text{Al}$ ), the dominant form in the uncalcined samples. Heat treatment of HT materials produces  $^{\text{IV}}\text{Al}$  sites as defects at the surface (Martínez-Ortiz *et al.*, 2008; Hibino and Tsunashima 1998; Debecker *et al.*, 2009); therefore, dye molecules reach these sites easily, thereby increasing the rate of adsorption.

The uptake curves for dye removal were obtained starting from solutions with different pH values (Figure 5). For the concentration range considered, the fastest rate and greatest degree of removal of dye occurred when acid solutions (pH 5.9 and 4) were used. A slight decrease in capacity and adsorption rates was

observed for solutions with basic pH (8.0). The initial pH of the dye solution is an important parameter for the adsorption process. The pH of the solution modifies the charge distribution at the surface of adsorbents as well as the degree of ionization of the solutes; this modifies the reaction kinetics and the equilibrium behavior of the adsorption processes. Dissolution of ionic dyes implies a release of colored charged species, and the adsorption of these charged groups onto the solid surface is influenced heavily by the surface charge of the solid. The dyes studied here behave as acids and upon dissolution they release anions which are the colored part of the molecule. Due to the positive electrical charge of the hydrotalcite and the anionic nature of both dyes, electrostatic forces facilitate the adsorption processes. In fact, the isoelectric point (IEP) for (MgAl)O mixed oxide is 10.9, as determined by Li *et al.* (2009). At pH values less than the IEP, the hydrated surface of the mixed metal hydroxide is positively charged. Under high pH values, acid sites at the solid surface, *e.g.* low coordinated Al, are assumed to be neutralized by  $\text{OH}^-$  anions coming from the solution, and the amount of sites available to retain the dye decreases. The rate of decrease in the number of adsorption sites is greater for sample MgAl-HT than for sample MgZnAl-HT. As mentioned, the adsorption sites on Zn-containing samples could be more varied in terms of acidic strength, *e.g.* Zn–O and Al–O, and this result seems to support this hypothesis.

The adsorption of DR is enhanced by the presence of Zn in the adsorbent (Figure 6). This kind of adsorbent is also able to remove almost all of the dye present in concentrations as low as 25 ppm.

The solids have a greater capacity to adsorb DR than ARBB. The plateau is reached when close to 60% of ARBB dye was retained in MgAl-HT, whereas close to 80% of the DR dye was retained on the same adsorbent under similar conditions.

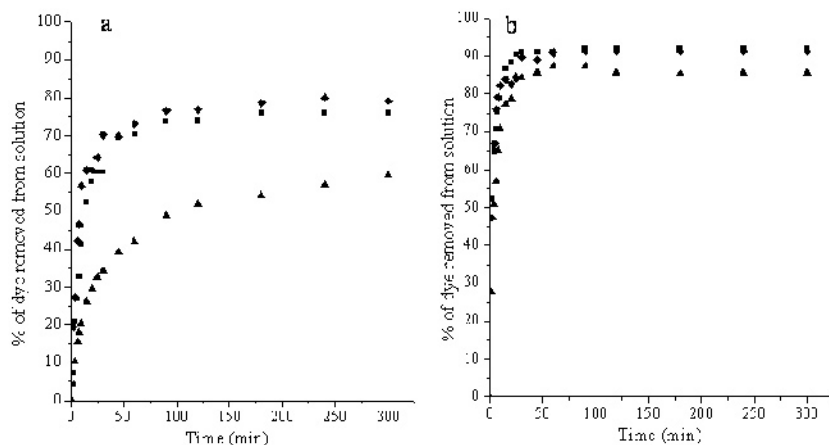


Figure 5. ARBB dye removed from 25 ppm solutions with time by adsorbents: (a) MgAl-HT, (b) MgZnAl. Solution pH at: 4 (◆), 5.9 (■), 8 (▲).

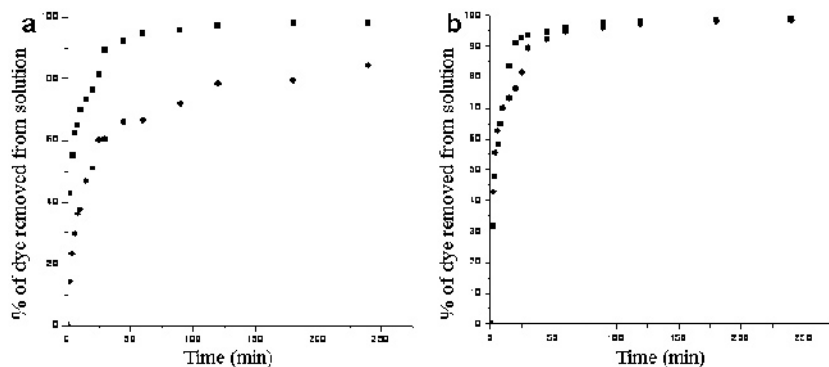


Figure 6. DR dye removed from solution as a function of time by adsorbents: (a) MgAl-HT, (b) MgZnAl. Initial dye concentrations (ppm): 25 (■), 50 (●). All solutions at pH 5.9.

*Adsorption kinetics.* The adsorption kinetics is an important feature in the control of the pollutant-removal process. To produce successful technological applications, the adsorption mechanism must be determined. Both kinetic and mechanistic aspects were considered here.

Adsorption kinetics can be modeled using the pseudo-first order (Lagergren and Svenska, 1898) and pseudo-second-order kinetics models (Ho and Chiang, 2001; Ho and McKay, 1999), given below as equations 1 and 2, respectively

$$\ln(q_e - q_t) = \ln q_e - k_1 t \tag{1}$$

$$\frac{t}{q_t} = \frac{1}{k_2 q_e^2} + \frac{1}{q_e} t \tag{2}$$

where  $k_1$  is the rate constant of the pseudo-first order adsorption ( $\text{min}^{-1}$ ),  $k_2$  is the rate constant of the pseudo-second-order adsorption ( $\text{g mg}^{-1} \text{min}^{-1}$ ), and  $q_e$  and  $q_t$  represent the amount of dye adsorbed ( $\text{mg g}^{-1}$ ) at equilibrium and at time  $t$ , respectively. By plotting  $t/q_t$

vs.  $t$  using the pseudo-second-order equation, the values of  $q_e$  and  $k_2$  can be calculated and  $k_2$  can be used to calculate the initial adsorption rate,  $h$  ( $\text{mg g}^{-1} \text{min}^{-1}$ ), as follows:

$$h = k_2 q_e^2 \tag{3}$$

The larger linear regression coefficients of the pseudo-second order kinetics model, compared to the pseudo-first order model, for removal of ARBB using the two layered materials MgZnAl-HT (Figure 7, Table 1) and MgAl-HT (Figure 8, Table 2) indicate that the experimental data are better described by the pseudo-second-order model. The  $q_e$  values calculated with this model are very close to those determined experimentally (Tables 1, 2). This behavior was independent of the experimental variables, *i.e.* adsorbent, dye, initial concentration, and pH. As expected, the initial adsorption rate was very dependent on the initial dye concentrations. Under the same conditions, adsorbents containing Zn showed greater initial adsorption rates than those adsorbents containing Mg and Al only,

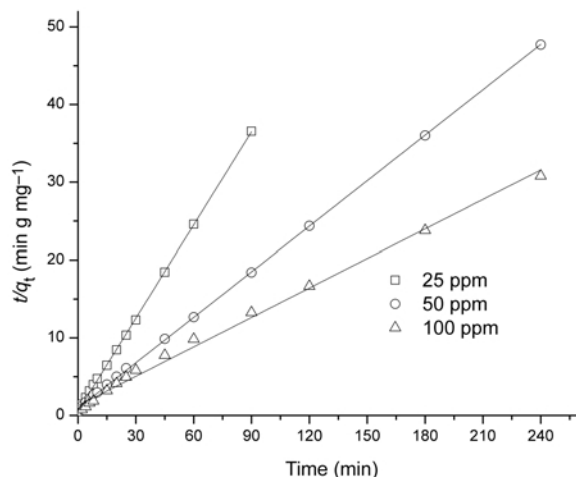


Figure 7. Plots of adsorption data for ARBB on MgZnAl-HT at pH 5.9 according to the pseudo-second-order rate equation 2.

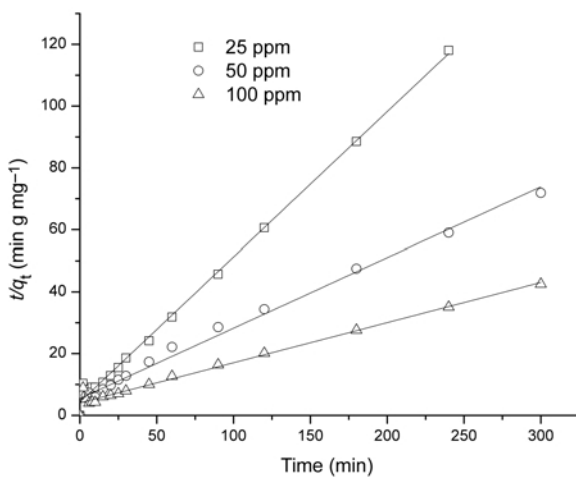


Figure 8. Plots of adsorption data for ARBB on MgAl-HT at pH 5.9 according to the pseudo-second-order rate equation 2.

Table 1. Kinetics values calculated for adsorption of ARBB and DR dyes onto layered and calcined materials at pH 5.9.

Dye system	Pseudo-first order model			Pseudo-second order model			$q_e$ (exp)	Initial adsorption rate ( $\text{mg g}^{-1} \text{min}^{-1}$ )
	$k_1$ ( $\text{min}^{-1}$ )	$q_e$ ( $\text{mg g}^{-1}$ )	$R^2$	$k_2$ ( $\text{g mg}^{-1} \text{min}^{-1}$ )	$q_e$ ( $\text{mg g}^{-1}$ )	$R^2$		
ARBB/MgAl-HT								
25 ppm	0.0207	9.90	0.900	$5.92 \times 10^{-3}$	21.41	0.998	19.10	2.649
50 ppm	0.0146	34.59	0.970	$9.56 \times 10^{-4}$	43.85	0.990	39.50	1.840
100 ppm	0.0146	59.12	0.978	$4.96 \times 10^{-4}$	75.18	0.991	68.25	2.805
ARBB/MgZnAl-HT								
25 ppm	0.0387	2.97	0.764	$3.71 \times 10^{-2}$	24.75	0.999	22.50	22.779
50 ppm	0.0216	20.96	0.926	$3.97 \times 10^{-3}$	51.28	0.999	45.15	10.440
100 ppm	0.0227	55.51	0.933	$1.24 \times 10^{-3}$	79.36	0.994	80.50	7.8340
ARBB/(MgAl)O								
50 ppm	0.0150	25.07	0.832	$3.92 \times 10^{-3}$	42.55	0.993	39.50	7.1022
ARBB/(MgZnAl)O								
50 ppm	0.0826	28.35	0.918	$5.63 \times 10^{-3}$	50.10	0.990	49.45	14.103
DR/MgAl-HT								
25 ppm	0.0152	14.23	0.949	$3.86 \times 10^{-3}$	21.83	0.996	24.80	1.8412
50 ppm	0.0097	26.73	0.943	$1.38 \times 10^{-3}$	39.52	0.993	41.52	2.1626
DR/MgZnAl-HT								
25 ppm	0.0193	6.72	0.749	$1.27 \times 10^{-2}$	25.83	0.999	24.75	8.8489
50 ppm	0.0252	20.90	0.959	$5.06 \times 10^{-3}$	48.78	0.999	49.75	12.0481

which supports the suggestion that the dye–adsorbent interactions are electrostatic.

**Adsorption mechanism.** Removal of dyes by adsorption processes can involve the following steps: (1) diffusion of the dye through the boundary layer; (2) intra-particle diffusion; and (3) adsorption of the dye on the adsorbent surface. In order to determine which step governs the overall adsorption process rate, the intra-particle-diffusion model was tested by Morris and Morris, (1963). This model relates the dye fraction uptake  $q_t$  at time  $t$  and  $K_{\text{int}}$ , the intra-particle-diffusion rate constant:

$$q_t = k_{\text{int}} t^{0.5} \quad (4)$$

For all dye-adsorbent systems analyzed here, plots of  $q_t$  vs.  $t^{0.5}$  showed a curve consisting of three linear sections. Such behavior confirms that intraparticle diffusion is not the only mechanism operative in the system. For the sake of conciseness, only one curve is drawn in Figures 9–10, indicating that three different, independent steps took place during the adsorption process, but only one was the rate-limiting step. The first and second linear sections are often related to external mass-transfer phenomena, whereas the third is due to the intra-particle diffusion. Thus, dye molecules are transported to the external surface of HTs, or their calcined derivatives, by film diffusion. The intra-particle diffusion coefficients,  $k_{\text{int},i}$ , under different conditions,

Table 2. Kinetics values calculated for adsorption of ARBB dye onto layered materials at 25 ppm.

Dye system	Pseudo-first order model			Pseudo-second order model			$q_e$ (exp)	Initial adsorption rate ( $\text{mg g}^{-1} \text{min}^{-1}$ )
	$k_1$ ( $\text{min}^{-1}$ )	$q_e$ ( $\text{mg g}^{-1}$ )	$R^2$	$k_2$ ( $\text{g mg}^{-1} \text{min}^{-1}$ )	$q_e$ ( $\text{mg g}^{-1}$ )	$R^2$		
ARBB/MgAl-HT								
pH = 4.0	0.0229	9.87	0.9134	$9.09 \times 10^{-3}$	20.44	0.9994	20.10	3.8037
pH = 5.9	0.0207	9.90	0.9001	$5.92 \times 10^{-3}$	21.41	0.9984	19.75	2.6490
pH = 8.0	0.013	11.85	0.9668	$2.88 \times 10^{-3}$	16.31	0.9946	15.25	0.7665
ARBB /MgZnAl-HT								
pH = 4.0	0.0773	8.67	0.9519	$3.2 \times 10^{-2}$	25.19	0.9997	22.75	20.3665
pH = 5.9	0.0387	2.97	0.7641	$3.71 \times 10^{-2}$	24.75	0.9999	22.70	22.7790
pH = 8.0	0.1115	16.76	0.9324	$1.55 \times 10^{-2}$	22.47	0.9967	21.50	7.8431

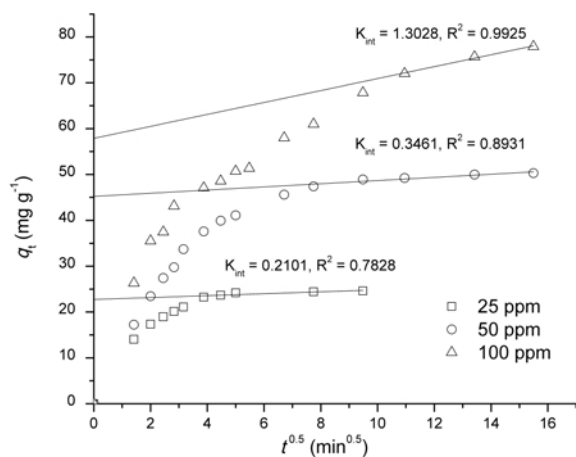


Figure 9. Plots of adsorption data for ARBB on MgZnAl-HT at pH 5.9 according to the intra-particle diffusion equation 4.

were calculated from the slopes of the corresponding linear sections (Figures 9 and 10). A greater slope might arise from an enhanced diffusion of dye molecules through porous systems. The pseudo-second-order rate constant,  $k_2$ , decreased with decreasing initial concentration (Table 1), meaning that the amount of dye removed would take longer for greater initial concentrations. Nevertheless, greater  $k_2$  values can be explained as the same amount of dye being removed more quickly.

*Adsorbents after dye adsorption.* The XRD patterns of neither the pure, uncalcined HTs, *i.e.* before adsorption (Figure 2a), nor the colored HTs after experiments with dye retention at pH 5.9 (Figure 11) showed any significant modifications, suggesting that the organic

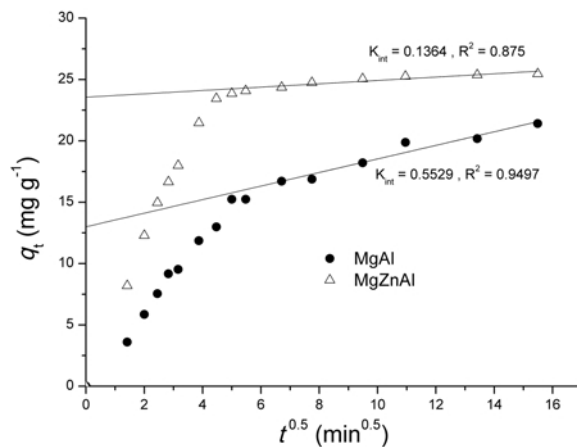


Figure 10. Plots of adsorption data for DR on MgAl-HT and MgZnAl-HT at 25 ppm and pH 5.9 according to the intra-particle diffusion equation 4.

dye was not intercalated between the brucite-like layers and destruction of the crystalline network did not occur as a consequence of the adsorption processes. On the contrary, mixed oxide with a periclase-like structure (Figure 2b) recovered the hydrotalcite-like structure after adsorption of dyes. Rehydrated and as-synthesized samples both contained the same peak due to the (003) plane at a similar position, *i.e.* 7.67 Å for rehydrated MgAl and 7.66 Å for fresh MgAl, indicating that recovery of the layered structure was only due to a rehydration of the oxides and carbonation of the interlayer for compensation of the charge (Veloso *et al.*, 2008; Prinetto *et al.*, 2000b). Intercalation of dyes does not occur because the (003) interlayer distance would be significantly larger if the dye had been

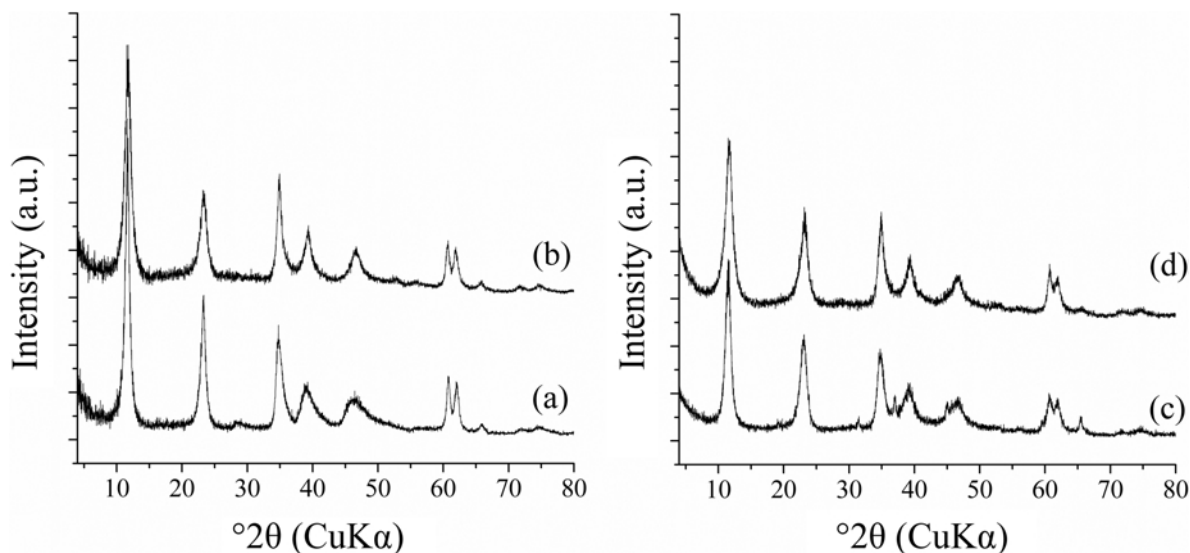


Figure 11. XRD patterns of adsorbents after dye retention (solution at pH 5.9 and concentration 100 ppm): (a) MgAl-HT, (b) MgZnAl, (c) (MgAl)O, and (d) (MgZnAl)O.



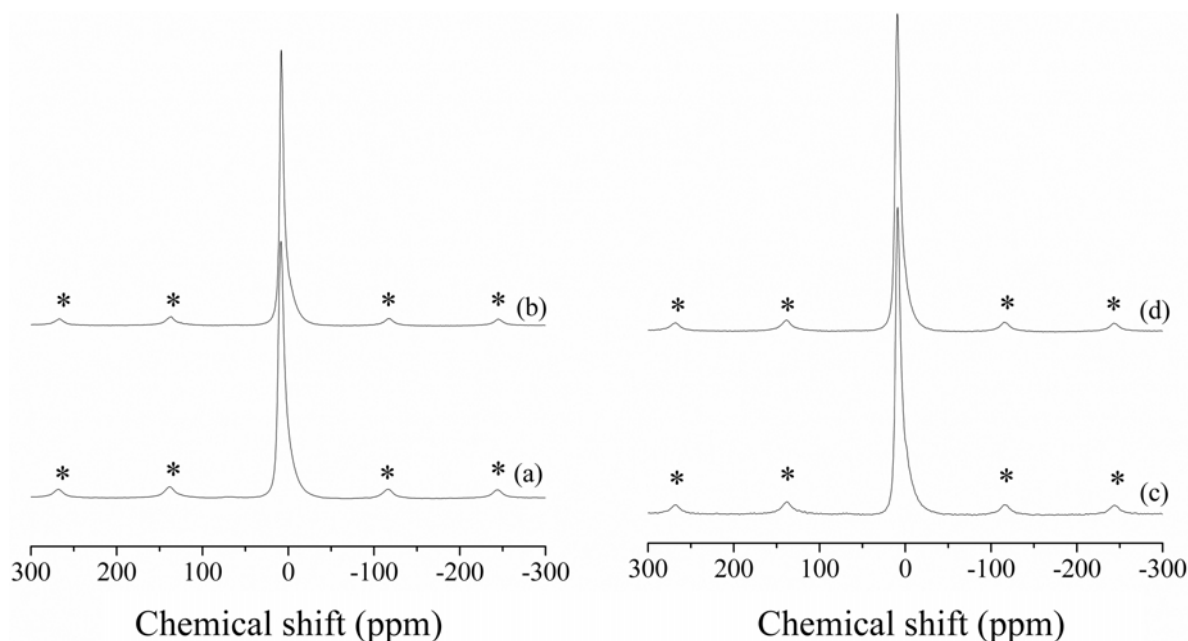


Figure 12.  $^{27}\text{Al}$  MAS NMR spectra of adsorbents after dye retention (solution at pH 5.9 and concentration 100 ppm): (a) MgAl-HT, (b) MgZnAl, (c) (MgAl)O, and (d) (MgZn)AlO. \* indicates spinning side bands (10 kHz).

incorporated between the layers. The  $^{27}\text{Al}$  MAS NMR spectra of both the mixed oxide and HT adsorbents after dye adsorption (Figure 12) show the typical signal due to octahedral Al at 5 ppm, suggesting that rehydration of mixed oxides was achieved by evolution in the coordination of Al, from four-fold to six-fold. The NMR signals of adsorbents after dye retention were very close to those of unheated HT samples. No strong interaction between Al ions and dye occurred either, in agreement with the previous suggestion that dye molecules were adsorbed at the surface through dipolar interactions. Such interactions are suitable for reversible adsorptions, meaning that the surface of the adsorbent can be regenerated and recycled.

### CONCLUSIONS

Layered and calcined carbonate-containing MgAl and MgZnAl hydrotalcite-like compounds exhibited potential for removal of ARBB and DR dyes from aqueous solutions. The removal was probably achieved by means of electrostatic interactions between the dye and the surface of the adsorbents. The presence of Zn enhanced the uptake capacity because it induced changes in the basicity of the adsorbent. The adsorption process was heavily dependent on the adsorbent, initial concentration of the dyes, and the pH. Results from adsorption kinetics indicated that the pseudo-second-order kinetics model described very well the adsorption of both dyes onto layered and calcined carbonate-containing MgAl and MgZnAl hydrotalcite-like compounds. The intraparticle diffusion model showed a multi-linear behavior suggest-

ing that the rate-controlling step may change during the adsorption process.

### ACKNOWLEDGMENTS

The authors thank CONACyT, SEP-PROMEP, and PAPIIT-UNAM for financial support *via* grants 128299, UAM-PTC-104, and IN107110, respectively. They also acknowledge Gerardo Cedillo and Adriana Tejada for their technical contributions.

### REFERENCES

- Bouraada, M., Belhafaoui, F., Ouali, M.S., and de Ménorval, L.C. (2009) Sorption study of an acid dye from an aqueous solution on modified Mg-Al layered double hydroxides. *Journal of Hazardous Materials*, **163**, 463–467.
- Choudhury, A.K. (2006) *Textile Preparation and Dyeing*. Science Publishers, New Hampshire, USA.
- Climent, M.J., Corma, A., Iborra, S., and Velty A. (2004) Activated hydrotalcites as catalysts for the synthesis of chalcones of pharmaceutical interest. *Journal of Catalysis*, **221**, 474–482.
- Constantino, U., Coletti, N., Nocchetti, M., Aloisi, G., and Elisei, F. (1999) Anion exchange of methyl orange into Zn-Al synthetic hydrotalcite and photophysical characterization of the intercalates obtained. *Langmuir*, **15**, 4454–4460.
- Debecker, D.P., Gaigneaux, E.M., and Busca G. (2009) Exploring, tuning and exploiting the basicity of hydrotalcites for applications in heterogeneous catalysis. *Chemistry – A European Journal*, **15**, 3920–3935.
- Deligeorgiev, T.G., Gadjev, N.I., Drexhage, K.H., and Sabnis, R.W. (1995) Preparation of intercalating dye thiazole orange and derivatives. *Dyes and Pigments*, **29**, 315–322.
- El Gaini, L., Lakraimi, M., Sebbar, E., Meghea, A., and Bakasse, M. (2009) Removal of indigo carmine dye from water to Mg-Al- $\text{CO}_3$ -calcined layered double hydroxides. *Journal of Hazardous Materials*, **161**, 627–632.

- El-Molla, M.M. and Schneider, R. (2006) Development of eco-friendly binders for pigment printing of all types of textile fabrics. *Dyes and Pigments*, **71**, 130–137.
- Figueras F. (2004) Base catalysis in the synthesis of fine chemicals. *Topics in Catalysis*, **29**, 189–196.
- Ganschow, M., Wörle, D., and Schulz-Eloff, G. (1999) Incorporation of differently substituted phthalocyanines into the mesoporous molecular sieve Si-MCM-41. *Journal of Porphyrins and Phthalocyanines*, **3**, 299–309.
- Herbst, W. and Hunger, K. (2004) *Industrial Organic Pigments*. Wiley-VCH Verlag & Co., Weinheim, Germany.
- Hibino, T. and Tsunashima, A. (1998) Characterization of repeatedly reconstructed Mg-Al hydrotalcite-like compounds: gradual segregation of aluminum from the structure. *Chemistry of Materials*, **10**, 4055–4061.
- Ho, Y.S. and Chiang, C.C. (2001) Sorption studies of acid dye by mixed sorbents. *Adsorption*, **7**, 139–147.
- Ho, Y.S. and McKay, G. (1999) Pseudo-second order model for sorption processes. *Process Biochemistry*, **34**, 451–465.
- Hoppe, R., Schulz-Ekloff, G., Wöhrle, D., Kirschhock, C., and Fuess H. (1994) Synthesis, location, and photoinduced transformation of zeolite-encaged thioindigo. *Langmuir*, **10**, 1517–1523.
- Hsiue, G.H., Lee, R.H., and Jeng, R.J. (1999) Organic sol-gel materials for second-order nonlinear optics based on melamines. *Journal of Polymer Science: Part A: Polymer Chemistry*, **37**, 2503–2510.
- Ibarra, I.A., Loera, S., Laguna, H., Lima, E., and Lara, V. (2005) Irreversible adsorption of an Aztec dye on fractal surfaces. *Chemistry of Materials*, **17**, 5763–5769.
- Inbaraj, B.S., Chiu, C.P., Ho, G.H., Yang, J., and Chen, B.H. (2006) Removal of cationic dyes from aqueous solution using an anionic poly-glutamic acid-based adsorbent. *Journal of Hazardous Materials*, **137**, 226–234.
- Johnson, C.A. and Glasser, F.P. (2003) Hydrotalcite-like minerals ( $M_2Al(OH)_6(CO_3)_{0.5} \cdot xH_2O$ , where  $M = Mg, Zn, Co, Ni$ ) in the environment: Synthesis, characterization and thermodynamic stability. *Clays and Clay Minerals*, **51**, 1–8.
- Jones, F. (1967) The color and constitution of organic molecules. Pp. 26–34 in: *Pigments: An Introduction to their Physical Chemistry*, (D. Patterson, editor). Elsevier, London.
- Lagergren, S. and Svenska, B.K. (1898) Zur theorie der sogenannten adsorption gelöster stoffe. *Vetenskapsakademien Handligar*, **24**, 1.
- Laguna, H., Loera, S., Ibarra, I.A., Lima, E., Vera, M.A., and Lara, V. (2007) Azoic dyes hosted on hydrotalcite-like compounds: Non-toxic hybrid pigments. *Microporous and Mesoporous Materials*, **98**, 234–241.
- Li, Y., Gao, B., Wu, T., Wang, B., and Li, X. (2009) Adsorption properties of aluminum magnesium mixed hydroxide for the model anionic dye Reactive Brilliant Red K-2BP. *Journal of Hazardous Materials*, **164**, 1098–1104.
- Lima, E., Bosch, P., Loera, S., Ibarra, I.A., Laguna, H., and Lara, V. (2009) Non-toxic hybrid pigments: Sequestering betanidin chromophores on inorganic matrices. *Applied Clay Science*, **42**, 478–482.
- Lippmaa, E., Samoson, A., and Magi, M. (1986) High-resolution 27Al NMR of aluminosilicates. *Journal of the American Chemical Society*, **108**, 1730–1735.
- Martínez-Ortiz, M.J., Lima, E., Lara, V., and Méndez Vivar, J. (2008) Structural and textural evolution during folding of layers of layered double hydroxides. *Langmuir*, **24**, 8904–8911.
- Morris, W.J. and Morris, J.C., (1963) Kinetics of adsorption on carbon from solution. *Journal of the Sanitary Engineering Division of the American Society for Civil Engineers*, **89**, 31–60.
- Orthman, J., Zhu, H.Y., and Lu, G.Q., (2003) Use of anion clay hydrotalcite to remove colored organics from aqueous solutions. *Separation and Purification Technology*, **31**, 53–59.
- Prinetto, F., Ghiotti, G., Durand, R., and Tichit, D. (2000a) Investigation of acid-base properties of catalysts obtained from layered double hydroxides. *Journal of Physical Chemistry B*, **104**, 11117–11126.
- Prinetto, F., Ghiotti, G., Graffin, P., and Tichit, D. (2000b) Synthesis and characterization of sol-gel Mg/Al and Ni/Al layered double hydroxides and comparison with co-precipitated samples. *Microporous and Mesoporous Materials*, **39**, 229–247.
- Rao, K.K., Gravelle, M., Sanchez Valente, J., and Figueras, F. (1998) Activation of Mg-Al hydrotalcite catalysts for aldol condensation reactions. *Journal of Catalysis*, **173**, 115–121.
- Rives, V. (2002) *Layered Double Hydroxides, Present and Future*. Nova Science, New York.
- Sampieri, A. and Lima, E. (2009) On the acid-base properties of microwave irradiated hydrotalcite-like compounds containing  $Zn^{2+}$  and  $Mn^{2+}$ . *Langmuir*, **25**, 3634–3639.
- Santos, S.C.R., Vilar, V.J.P., and Boaventura, R.A.R. (2008) Waste metal hydroxide sludge as adsorbent for a reactive dye. *Journal of Hazardous Materials*, **153**, 999–1008.
- Thevenot, F., Szymanski, R., and Chaumette, R. (1989) Preparation and characterization of Al-rich Zn-Al hydrotalcite-like compounds. *Clays and Clay Minerals*, **37**, 396–402.
- Tunç, Ö., Tanac, H., and Aksu, Z. (2009) Potential use of cotton plant wastes for the removal of Remazol Black B reactive dye. *Journal of Hazardous Materials*, **163**, 187–192.
- Valente, J., Sánchez-Cantú, M., Lima, E., and Figueras, F. (2009) Method for large-scale production of multimetallic layered double hydroxides: formation mechanism discernment. *Chemistry of Materials*, **21**, 5809–5818.
- Veloso, C.O., Noda Pérez, C., de Souza, B.M., Lima Ev., C., Dias, A.G., Monteiro, J.L.F., and Henriques, C.A. (2008) Condensation of glyceraldehyde acetonide with ethyl acetoacetate over Mg, Al-mixed oxides derived from hydrotalcites. *Microporous and Mesoporous Materials*, **107**, 23–30.
- Vigo, T.L. (1994) *Textile Processing and Properties: Preparation, Dyeing, Finishing and Performance*. Elsevier, New York.
- Wark, M., Ganschow, M., Ortlam, A., Schulz-Ekloff, G., and Wöhrle, D. (1998) Monomeric encapsulation of phthalocyanine dye molecules in the pores of Si-MCM-41 and Ti-MCM-41. *Journal of Physical Chemistry - Berichte der Bunsen-Gesellschaft*, **102**, 1548–1553.
- Wu, F., Tseng, R., and Juang, R. (2001) Kinetic modeling of liquid-phase adsorption of reactive dyes and metal ions on chitosan. *Water Research*, **35**, 613–618.
- Zhu, M., Li, Y-P., Xie, M., and Xin, H-Z. (2005) Sorption of an anionic dye by uncalcined and calcined layered double hydroxides: a case study. *Journal of Hazardous Materials*, **120**, 163–171.

(Received 7 March 2011; revised 8 August 2011; Ms. 511; A.E. L.B. Williams)